# Scintillometer Wind Measurements over Complex Terrain

LIONEL P. POGGIO,* MARKUS FURGER, ANDRÉ S. H. PRÉVÔT, AND WERNER K. GRABER

*Atmospheric Pollution Section, Paul Scherrer Institute, Villigen, Switzerland*

EDGAR L ANDREAS

*U.S. Army Cold Regions Research and Engineering Laboratory, Hanover, New Hampshire*

(Manuscript received 6 October 1998, in final form 29 March 1999)

ABSTRACT

Several large-aperture scintillometers were built at the Paul Scherrer Institute with the aim to measure wind over complex terrain. A prototype instrument was tested over flat ground, and the performance of six analyzing techniques was evaluated by comparing them with conventional anemometers. Next, a set of five improved scintillometers was used in an experiment over complex terrain. This experiment represents a unique opportunity for evaluating scintillometer performance by comparing their results to sodar, aircraft, and ground station measurements. The results complement and partly contradict the observations previously published; the so-called peak technique is the most reliable and frequency techniques fail to provide faithful results in many cases. The measurements demonstrate that scintillometry is useful and reliable for wind and turbulence measurements over complex terrain.

## 1. Introduction

Optical remote sensing is an appealing method to measure wind in complex terrain. The Paul Scherrer Institute (PSI) uses a combination of scintillometers and Differential Optical Absorption Spectrometer (DOAS) systems to measure fluxes of various gases over complex terrain. Each instrument observes a distant light source to infer meteorological and chemical data. The scintillometer measures the wind component perpendicular to an infrared light beam by observing its scintillation. The DOAS evaluates concentrations of $NO_2$, $O_3$, toluene, and $SO_2$ by measuring the differential absorption of UV light at different wavelengths.

To better understand the complex flow structure in a valley, it is necessary to have continuous measurements of meteorological parameters not only at the ground but also at elevated levels within the valley atmosphere. Optical instruments can measure high above the valley floor where other measurement platforms are either available only for short periods or are very expensive.

Scintillometry has been studied for more than 30 years and is a valuable method to investigate the atmosphere. Its advantage is that it yields integral, remotely sensed measurements of either crosswind speed or turbulence parameters over distances up to several kilometers. Using scintillation for wind measurements originated with astronomical observations (Briggs et al. 1950), was developed for use with artificial light sources in the 1960s and 1970s (i.e., Lawrence et al. 1972), and is still in use (i.e., Wang and Crosby 1996). Determining turbulence parameters such as the refractive index structure coefficient $C_n^2$ and the inner scale of turbulence, $l_0$, also yields turbulent fluxes (Andreas 1991; de Bruin et al. 1995; Hill 1997). Path averaging provides more representative measurements and leads to data that are statistically more stable even for short averaging times. Scintillometers do not induce flow distortion and can run continuously with only occasional servicing. Although scintillometry has been tested mainly over flat, homogeneous areas, it could be very helpful for measurements on airport runways, in a valley (Porch et al. 1988), or over water (de Jong and de Leeuw 1997).

## 2. Crosswind scintillometry

### *a. Measurement techniques*

The instrument observes a distant light source to measure the wind. Typically, two detectors are placed in a light beam. The detectors are separated by the distance $\rho$. Light-sensitive detectors register the scintillation as

* Additional affiliation: Institute for Atmospheric Science, ETH, Zurich, Switzerland.

*Corresponding author address:* Dr. Markus Furger, Paul Scherrer Institute, 5232 Villigen PSI, Switzerland.
E-mail: markus.furger@psi.ch

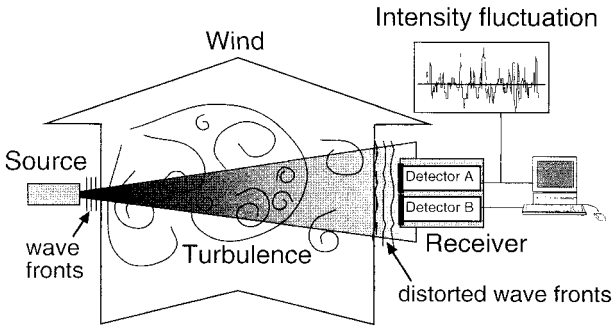


FIG. 1. Schematic diagram of a scintillometer. The receiver typically consists of two light-sensitive detectors separated by the distance $\rho$.

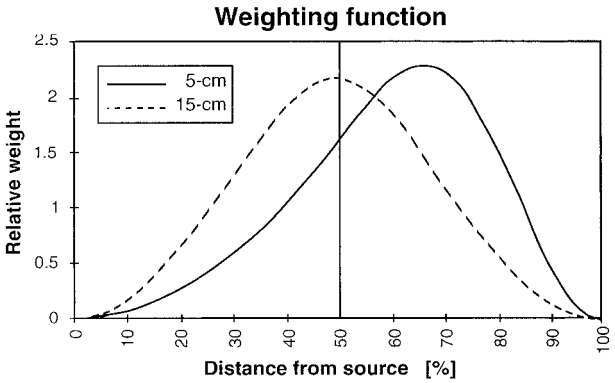


FIG. 2. Weighting functions for a 15-cm transmitter aperture, and 5- and 15-cm receiving apertures. The distance from the source is given in percent of the pathlength.

intensity fluctuations, and the signal is processed to determine the wind component perpendicular to the light beam (Fig. 1). The scintillation is caused by drifting refractive-index irregularities in the atmosphere. These irregularities are due to atmospheric turbulence, and turbulence can be visualized as consisting of irregular swirls of motion. These motions are called eddies. The result of the scintillometer measurement is a weighted average over the pathlength. The weighting functions for the instruments built at PSI are plotted in Fig. 2.

Optical crosswind techniques are thoroughly described by Wang et al. (1981). Theoretical analyses of scintillation lead to several different evaluation techniques. We compare six different methods and report the results of these tests here.

The wind-sensing methods can be grouped into two categories: covariance and frequency techniques. Covariance techniques use the readings from two detectors; computing and analyzing the time-lagged covariance function provide both wind speed and wind direction. Frequency techniques relate the frequency of one fluctuating signal to the wind strength but cannot determine the wind direction.

### 1) COVARIANCE TECHNIQUES

Covariance techniques use the analysis of the normalized time-lagged covariance function, $C(\tau)$ (Fig. 3). Here $C(\tau)$ is based on the measurements of the two detectors A and B. The receiver records the intensity $I_A(t)$ and $I_B(t)$, so we get for $C(\tau)$

$$C(\tau) = \frac{\int_{t1}^{t2} [I_A(t+\tau) - \overline{I_A}][I_B(t) - \overline{I_B}]\, dt}{\sqrt{\int_{t1}^{t2} [I_A(t) - \overline{I_A}]^2\, dt \int_{t1}^{t2} [I_B(t) - \overline{I_B}]^2\, dt}}. \quad (1)$$

The time span $t_1$–$t_2$ used for our measurements was 1 s.

The covariance function suggests three ways to estimate the wind speed.

1) *Slope technique.* The crosswind $V$ is proportional to the slope $S$ at zero delay of the cross-covariance curve

$$V \sim S. \quad (2)$$

The slope technique was developed by Lawrence et al. (1972).

2) *Peak technique.* The crosswind can be obtained from the time delay at the peak of the cross-covariance curve, $\tau_P$:

$$V \sim 1/\tau_P. \quad (3)$$

This technique simply relates $V$ to the time needed by a scintillation pattern to drift from one detector to the other.

3) *Briggs technique.* The crossover time delay of the autocovariance and cross-covariance curves, $\tau_B$, is inversely proportional to $V$:

$$V \sim 1/\tau_B. \quad (4)$$

This technique was first used by astronomers to de-

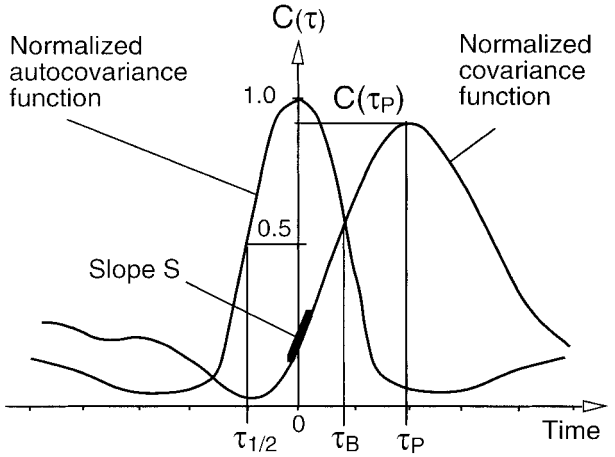


FIG. 3. Typical normalized cross-covariance and autocovariance curves. The variables $S$, $\tau_P$, $\tau_{1/2}$, and $\tau_B$ are defined in the text.

termine stratospheric wind from stellar scintillation (Briggs et al. 1950).

Since different portions of the path contribute to the scintillation pattern, that pattern evolves continuously because of the relative speeds of the different-sized features it contains. Nonuniformity in the wind or in the strength of turbulence will increase the rate of loss of correlation in the scintillation pattern as it drifts from one detector to the next. The scintillation pattern also evolves due to the decay of the turbulence eddies themselves. The value of the covariance function at time $\tau_P$, $C(\tau_P)$, will be used to quantify the loss of correlation in the scintillation pattern and, therefore, the quality of the measurements.

#### 2) FREQUENCY TECHNIQUES

Frequency techniques are based on the frequency of intensity fluctuations, $\tilde{f}$, of one signal and cannot discern wind direction. The crosswind is proportional to the frequency of the signal:

$$|V| \sim \tilde{f}. \tag{5}$$

We consider three ways to characterize the frequency of the intensity fluctuations.

1) *Autocorrelation technique.* The width of the autocovariance curve, $\tau_{1/2}$, is inversely proportional to $\tilde{f}$ (Fig. 3):

$$\tilde{f} = 1/\tau_{1/2}. \tag{6}$$

2) *Fast Fourier transform (FFT) technique.* We determine the Fourier transform $W(f)$ of the signal; the principal frequency $f_{\max}$ is the frequency for which $W(f)$ shows its maximum. Then

$$\tilde{f} = f_{\max}. \tag{7}$$

3) *Zero-cross technique.* This frequency measurement is made by counting the number of times the fluctuating signal crosses the mean of the signal:

$$\tilde{f} = \text{count}. \tag{8}$$

The theory developed by Wang et al. (1981) describes scintillation phenomenon fairly satisfactorily but makes two assumptions that can lead to discrepancies between theoretical predictions and experimental results. First, Wang et al. assume that the turbulence spectrum follows a universal form and that this spectrum does not vary with time. Second, they assume Taylor's ''frozen turbulence'' hypothesis. Taylor's hypothesis is that the turbulent eddies do not change significantly during the time they drift through the light beam.

The performance of the different techniques has been theoretically and experimentally tested before. The peak technique is reported to be less accurate than the slope technique because the scintillation pattern decorrelates as it drifts past the sensors (Wang et al. 1981; Eaton et al. 1990). Frequency techniques have also been reported to be more accurate than covariance techniques (Wang et al. 1981). Some methods of evaluation use frequency techniques to determine the wind speed and covariance techniques to resolve wind direction (Biltoft 1989).

### *b. Hardware*

A prototype scintillometer based on the model of Wang et al. (1981) was built at PSI. This instrument uses, as a light source, an infrared diode that operates with a peak wavelength between 0.8 and 0.9 $\mu$m. Transmitter and receiver apertures have diameters of 15 and 5 cm, respectively. The spacing between the centers of the two receiver apertures is 6.3 cm. The signal intensity was stored with a sampling rate of 500 Hz on a portable computer, and data processing was subsequently done offline on a mainframe computer.

Next, six instruments with larger-aperture receivers were built. Each receiver has three 15-cm spherical mirrors arranged in an L shape for measuring both horizontal and vertical wind components. We will report only measurements of the horizontal wind component. The incoming light is reflected onto a detector placed at the focal point of the corresponding mirror. The spacing between the centers of adjacent detectors is 17.2 cm. The instrument uses the same transmitter as the prototype. Because of the larger optics, this instrument can be used over longer distances. For example, we tested this instrument in 1997 over a 6.5-km path.

## 3. Experiment over flat ground

During the summer of 1994, the prototype scintillometer was placed on a 1-km path over flat terrain near Würenlingen, Switzerland. The transmitter and receiver were installed on platforms 3.5 m above ground. Nine automatic meteorological stations with conventional cup anemometers were set up along the light path at the same height as the light path. The data from the conventional anemometers were averaged over 5 s and then used as a reference for comparing with the scintillometer data. The wind component measured with the conventional anemometers will be referred to as $V_G$. The parameters calculated from the scintillation measurements were $S$, $\tau_P$, $\tau_B$, $\tau_{1/2}$, the variable ''count,'' and $f_{\max}$, as described before. Additionally, $C(\tau_P)$ was calculated.

Table 1 shows that increasing averaging times leads to a better performance of all the evaluation techniques, especially the peak technique because averaging minimizes the influence of failures in the detection scheme and improves the signal-to-noise ratio by low-pass filtering. Failures often happen when wind and turbulence are weak; the covariance function is then not well defined, and its peak is close to zero. As a result, the peak technique gives unrealistically high values for the wind, while the slope technique gives values near zero, fortuitously close to reality.

TABLE 1. Correlation coefficients between the conventional anemometers and the prototype scintillometer for six different techniques and for different averaging times. Measurements were on 25 Jul 1994.

| Technique | Averaging time | | |
|---|---|---|---|
| | 5 s | 1 min | 10 min |
| Slope | 0.84 | 0.89 | 0.94 |
| Peak | 0.79 | 0.93 | 0.97 |
| Briggs | 0.88 | 0.94 | 0.97 |
| Autocorrelation | 0.96 | 0.98 | 0.99 |
| FFT | 0.93 | 0.97 | 0.99 |
| Zero-cross | 0.96 | 0.98 | 0.99 |

TABLE 2. Correlation ($r$) and standard deviation ($\sigma$), in m s$^{-1}$, of the difference between the prototype scintillometer and the conventional anemometers. The values in boldface taken on 10 Aug show lower correlation caused by rain. The calculations are based on 1-min averaged measurements.

| | 25 Jul 94 | | 10 Aug 94 | | 23 Aug 94 | |
|---|---|---|---|---|---|---|
| | $r$ | $\sigma$ | $r$ | $\sigma$ | $r$ | $\sigma$ |
| Slope | 0.89 | 0.29 | 0.94 | 0.21 | 0.88 | 0.21 |
| Peak | 0.93 | 0.24 | 0.93 | 0.23 | 0.93 | 0.17 |
| Briggs | 0.94 | 0.22 | 0.96 | 0.30 | 0.90 | 0.22 |
| Autocorrelation | 0.98 | 0.14 | **0.84** | **0.29** | 0.94 | 0.13 |
| FFT | 0.97 | 0.15 | 0.94 | 0.17 | 0.94 | 0.13 |
| Zero-cross | 0.98 | 0.13 | **0.65** | **0.47** | 0.94 | 0.14 |

This experiment was used to test and calibrate the six evaluation techniques described earlier. Figure 4 shows sample measurements from 25 July 1994. The data presented in Fig. 4, and in the remaining figures of this paper, are averaged over 10 min, while Table 2 is based on 1-min averages. The correlation between the scintillometer and the conventional anemometers is given in Table 2 for three different experiments, each lasting over 12 h. The performance of the peak technique is at least as good as the slope technique, contradicting the results found in the literature (Wang et al. 1981). The wind speed deviation is about 0.15 m s$^{-1}$ for the frequency techniques and 0.25 m s$^{-1}$ for the covariance techniques in the wind speed range of up to 2 m s$^{-1}$. This yields relative errors of 7.5% for the frequency techniques and 12.5% for the covariance techniques. These numbers agree with measurements in higher wind speed ranges (up to 8 m s$^{-1}$). Our results indicate that the frequency techniques are more precise than the covariance techniques. The three different techniques used to determine the frequency content of the intensity fluctuation show the same performance and the same characteristics. But the relation between frequency techniques and wind speed does not seem to be linear (Fig. 5).

The proportionality factors in the relations (2)–(8) were determined experimentally. To fit the data better, however, we rewrite the relation (5) as

$$|V| \sim \tilde{f}^{\alpha}, \tag{9}$$

where $\alpha = 1.8$ for the autocorrelation technique, $\alpha = 2$ for the zero-cross technique, and $\alpha = 2.3$ for the FFT technique. The need to introduce the exponent $\alpha$ can be explained as a failure of Taylor's hypothesis. The turbulence eddies do decay as they cross the beam; the resulting intensity decorrelation is proportional to the time delay. The frequency techniques consequently overestimate the wind. This overestimation becomes greater as the wind decreases. Introducing (9) counterbalances this effect and provides agreement between anemometer and scintillometer winds.

The effect of loss of correlation can be seen if we consider the peak value of the correlation function, $C(\tau_P)$. Loss of correlation can be caused by inhomogeneities of the atmosphere along the path, the nonlinear interaction among the eddies, and by violations of Taylor's hypothesis (Hill 1996). Wang et al. (1981) neglect turbulence decay and take account only of inhomogeneities of the wind and in the strength of the turbulence along the path to explain the evolution of the scintillation pattern during its drift past the receiver. The loss of correlation, however, can be quantified by the mea-

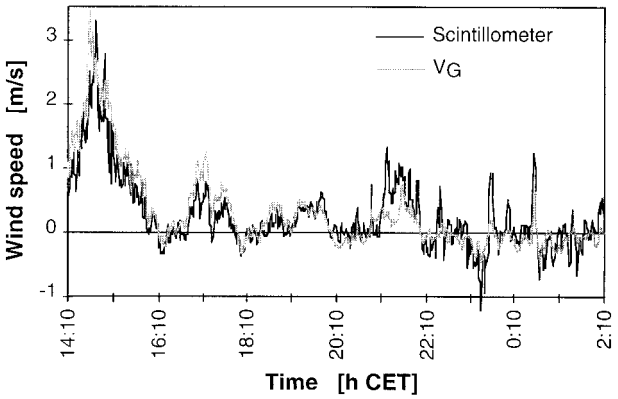


FIG. 4. Scintillometer measurements (slope technique) compared to the spatially averaged measurement of nine conventional anemometers ($V_G$). The measurements started at 1410 CET 25 Jul 1994 and lasted 12 h.

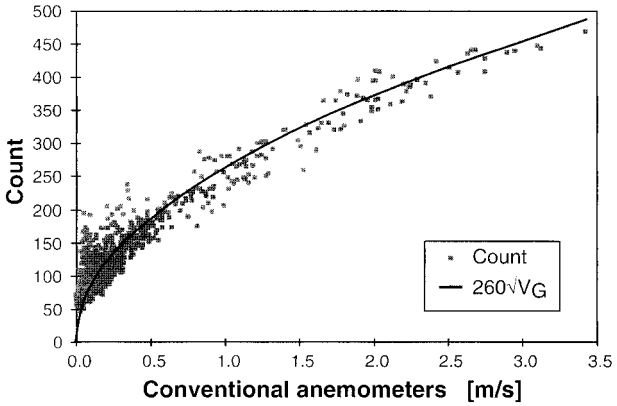


FIG. 5. Relation between "count" and wind speed. The variable "count" seems to be proportional to $|V_G|^{1/2}$.

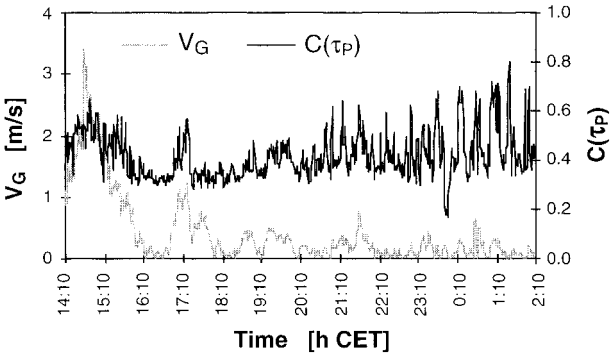


FIG. 6. The $C(\tau_P)$ for the measurement on 25 Jul 1994 together with the wind speed measured with the conventional anemometers, $V_G$.

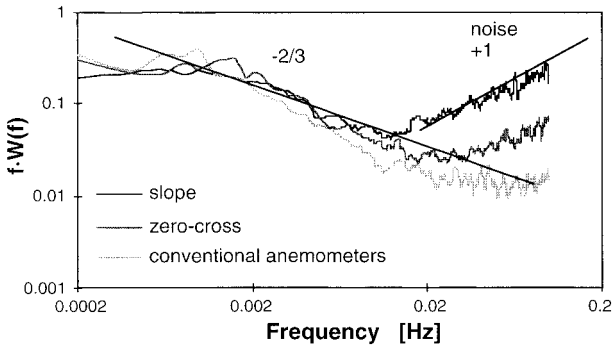


FIG. 7. Normalized spectra, calculated for 12 h on 25 Jul 1994, from the conventional anemometers and from scintillometer winds obtained with the slope and zero-cross techniques.

surement of the maximum of the covariance function, $C(\tau_P)$. The covariance function shows maxima between 0.3 and 0.8 (Fig. 6). During the afternoon, $C(\tau_P)$ reaches values up to 0.6, when the wind is stronger. After sunset, $C(\tau_P)$ reaches values up to 0.7–0.8 despite the facts that the wind speed stays very low and no change in the homogeneity of the wind field could be detected.

For the first four hours of the measurements (afternoon), we observe a good correlation between $C(\tau_P)$ and the wind speed; the values of $C(\tau_P)$ then become larger during the nighttime, while the wind speed falls (Fig. 6). If we consider only the nighttime period, we see that the correlation between $C(\tau_P)$ and the wind speed is also good during that time. We speculate that the relation between $C(\tau_P)$ and wind speed changes because the atmospheric turbulence changes. In the strongly turbulent afternoon atmosphere, the largest eddies are larger and the smallest eddies are smaller than in the stably stratified, weakly turbulent nighttime atmosphere. Thus, the turbulence spectra have different shapes and levels during the day and at night. The correlation of the scintillation pattern also decays more rapidly during the day than at night because increasing turbulence intensity causes more serious violations of Taylor's approximation that the scintillation pattern moves coherently with the mean flow (Wyngaard and Clifford 1977; Hill 1996). The overall effect on our measurements is that the calibration factors are different in weak and strong turbulence with the result that covariance techniques overestimate the wind speed at night.

We have taken the Fourier transform of scintillometer wind data from a 12-h period on 25 July 1994 and computed the spectral density $W(f)$. Figure 7 shows the typical $-\frac{2}{3}$ Kolmogorov roll-off of $fW(f)$. The influence of noise is obvious for frequencies larger than 0.01 Hz for the slope technique and 0.02 Hz for the zero-cross technique. This confirms the better performance of the frequency techniques for the experiment over flat ground.

Rain influenced one of our measurement periods (Table 2). Autocorrelation and zero-cross techniques overestimate the wind speed during that period. In effect, the additional scintillation caused by falling raindrops is interpreted as extra velocity. The other four evaluation techniques seem unaltered by the rain, except perhaps for the larger standard deviation with the Briggs technique.

## 4. Experiment over complex terrain

### *a. Introduction*

In 1996, PSI participated in Vertical Ozone Transport in the Alps (VOTALP) with a set of five scintillometers. VOTALP is a European Union research project to study the production and transport of ozone in the Alps (Furger et al. 1997; Wotawa et al. 1996). PSI contributes with various measurement systems and performs model calculations. The influence of thermal circulation on ozone concentrations and on the exchange of ozone between the valley atmosphere and the free troposphere aloft was the main focus of the valley campaign in the summer of 1996 in southern Switzerland. The measurements made with the scintillometers should help investigate questions relevant to the project. This experiment also was an opportunity to evaluate the performance of the scintillometers over complex terrain by comparing their measurements with aircraft, sodar, and ground station measurements.

The Mesolcina Valley in southern Grisons, Switzerland, was selected as the site for the valley experiment. This valley is oriented approximately north–south. It has relatively smooth sidewalls without major tributary valleys (except the Calanca Valley at the southern end). By measuring the airflow across two planes perpendicular to the valley axis, it is possible to obtain an estimate of the amount of air entering or exiting the valley. During the VOTALP experiment, the PSI scintillometers were used for the first time in complex terrain where inhomogeneities in wind and turbulence can distort the measurements.

Comparisons with ground measurements provide some qualitative information about the accuracy of the

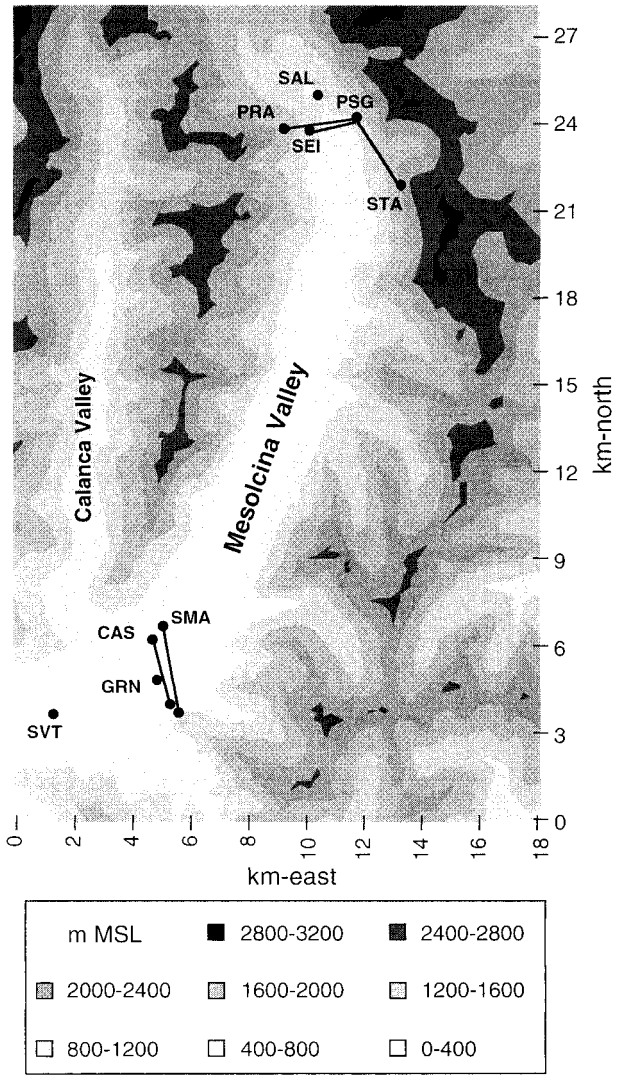


FIG. 8. Experimental setup in the Mesolcina valley. See text for acronyms. (Digital Terrain Model data reproduced with the permission of the Swiss Federal Office of Topography, dated 24 Sep 1998.)

scintillometer measurements. Measurements obtained with an aircraft provide another opportunity to check the accuracy of the scintillometers and to evaluate the homogeneity of the wind field. This comparison, however, is available only for limited periods. The sodar measurements allow comparisons over longer periods.

### b. Experiment setup

PSI installed five scintillometer/DOAS systems in the Mesolcina Valley (Fig. 8). Two scintillometers were set across the southern end of the valley with their receivers in Castaneda (CAS) and Santa Maria (SMA) and their transmitters on the other side of the valley. Two scintillometers were placed across the northern end with receivers in Sei (SEI) and Pradiron (PRA) and both transmitters in Pian San Giacomo (PSG). One scintillometer was parallel to the valley sidewall with its receiver in Stabi (STA) and transmitter in Pian San Giacomo. Beam lengths ranged from 0.9 to 2.7 km (Table 3). The intensity fluctuations were recorded at a rate of 2 kHz, generating about 1.2 Gbytes of data for each instrument every day. The signal was then processed and the wind speed determined with the different techniques described above. For the scintillometers set across the valley, positive measurements made with the covariance techniques represent down-valley wind; negative values represent up-valley winds.

TABLE 3. List of optical paths deployed during the VOTALP valley experiment. The given height is the distance to the ground at the path center.

| Path name | Length (km) | Height (m) |
|---|---|---|
| Castaneda (CAS) | 2.3 | 400 |
| Santa Maria (SMA) | 2.7 | 600 |
| Pradiron (PRA) | 1.6 | 250 |
| Sei (SEI) | 0.9 | 60 |
| Stabi (STA) | 2.1 | 250 |

Surface observations were available in Santa Maria, Grono, Pian San Giacomo, Pradiron, Salec (SAL), and Stabi. A sodar was placed in San Vittore (SVT). The company MetAir AG conducted aircraft measurements. These measurements comprised six days: 19, 22, and 23 July; and 16, 17, and 18 August. The aircraft performed about seven flight hours each day, typically in two periods: from 1000 to 1300 and from 1500 to 1830 central European time (CET).

### c. Measurement of $C(\tau_P)$

Measurements of $C(\tau_P)$ give a first indication about the quality of the data and help classify them into different periods. During the day, scintillation is strong and correlated with the incoming solar radiation. During the night, the scintillation can also be quite strong, but scintillation is induced by wind shear and temperature gradients. Periods of transition between nighttime and daytime conditions are characterized by very weak scintillation, weak winds, and low values of $C(\tau_P)$. During those periods, the wind measurements may be questionable. The highest values of $C(\tau_P)$ occur during the night for the path at Sei. Values get as low as 0.2 during transition periods (Fig. 9). For the paths at Castaneda and Santa Maria, the values of $C(\tau_P)$ range between 0.4 and 0.6. For Stabi, the values are between 0.2 and 0.4 due to the fact that the flow is not horizontal. The $C(\tau_P)$ correlates with the wind speed; that is, the smaller the wind speed, the smaller $C(\tau_P)$.

### d. Wind measurements

#### 1) COMPARISON AMONG THE TECHNIQUES

Wind speed can be computed from raw scintillometer data with any of the methods described in section 2.

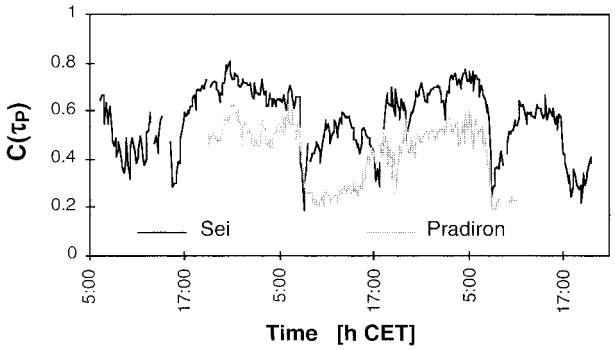


FIG. 9. Maximum values of the correlation function, $C(\tau_P)$, for the Sei and Pradiron paths, 16–18 Aug 1996.

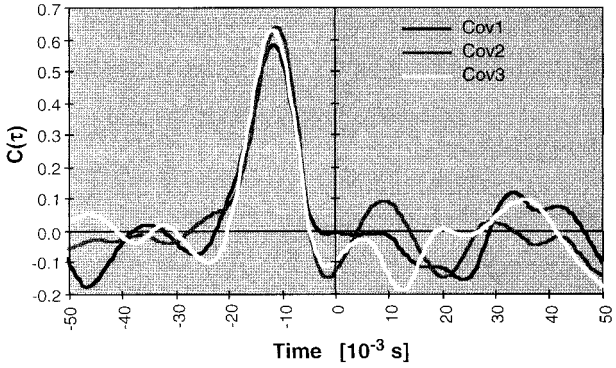


FIG. 11. Three covariance functions measured at Santa Maria in the afternoon of 18 Aug for three consecutive seconds.

Although these methods should give the same results, discrepancies appear during certain periods. We systematically compared all techniques except for the Briggs technique and found that the frequency techniques (FFT, zero-cross, and autocorrelation) yielded identical results, while the covariance techniques (peak and slope) revealed discrepancies in some sitations. We compared the scintillometer crosswind measurements to both conventional anemometer wind components parallel and perpendicular to the light beam, but we could not find any correlation between the parallel component and the degradation of the scintillometer measurements in complex terrain. The degradation of the scintillometer measurements was quantified by the standard deviation of the difference between the scintillometer crosswind and the anemometer wind component perpendicular to the light beam (Table 2). The same was true for our experiments over flat terrain.

For example, the peak technique gives higher values than the slope technique for the Pradiron path. Low $C(\tau_P)$ values yield an underestimation of the wind by the slope technique compared to the peak technique.

Large discrepancies between the slope and peak method also occur for the Castaneda and Santa Maria paths during the daytime (Fig. 10). Except for the afternoon of 15 August, the peak technique shows values two to three times larger than the slope technique. Typical covariance functions are shown in Fig. 11. The peak of the function is well defined, and evaluations of the wind speed with the peak technique for each curve give approximately $-3.5$ m s$^{-1}$, while the slope technique gives 0.3, 1.5, and 0.4 m s$^{-1}$. The shape of the covariance function indicates that the slope technique is not appropriate for the wind measurements during this period. Possibly, strong turbulence (i.e., high $C_n^2$ values) near the transmitter or receiver end of the light path is responsible for this behavior, but we do not have independent turbulence measurements to test this hypothesis.

Discrepancies between covariance and frequency techniques also appear. In the case of Santa Maria and Castaneda, the frequency techniques agree well with the covariance techniques during the day, but the frequency techniques show unrealistically small values during the night. Specifically, wind speeds from the autocorrelation technique are much lower than for the peak technique during the night and are very close during the afternoon and on the last night (Fig. 12). Discrepancies between the different evaluation techniques have their origin in changes in the turbulence spectrum of the atmosphere.

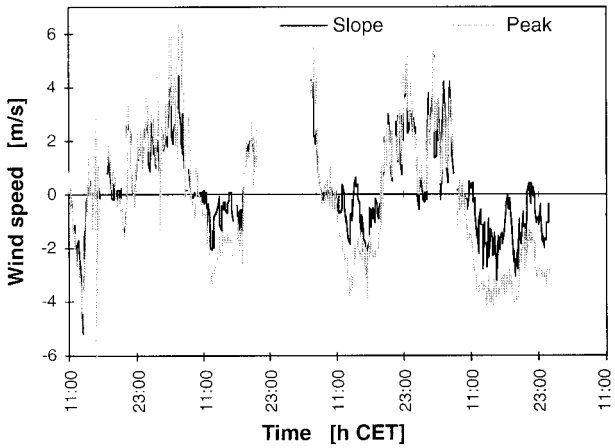


FIG. 10. Comparison between the slope and peak techniques for Santa Maria, 15–19 Aug 1996.

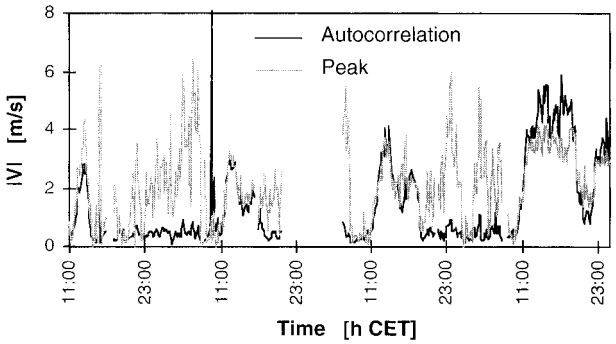


FIG. 12. Comparison of the peak and autocorrelation techniques for Santa Maria, 15–19 Aug 1996.

TABLE 4. Correlation between the scintillometer path at Sei and the ground stations in Salec (SAL) and Pian San Giacomo (PSG). The last two hours of measurements are ignored because of obvious instrument failure (355 data points).

| | Slope | Peak | PSG | SAL |
|---|---|---|---|---|
| Slope | 1.00 | | | |
| Peak | 0.97 | 1.00 | | |
| PSG | 0.93 | 0.93 | 1.00 | |
| SAL | 0.92 | 0.93 | 0.87 | 1.00 |

### 2) COMPARISON WITH GROUND STATIONS

For Sei and Pradiron, the correlation with the ground stations is good (Tables 4, 5). The scintillometers indicate stronger winds than the ground stations during the night (Fig. 13). We notice that the peak technique measurements are better correlated to the ground station measurements than the slope technique measurements. For the Santa Maria and Castaneda paths, the scintillometers measure stronger winds than the ground stations during both night and day. However, the correlation between scintillometers and ground stations is good (Table 6).

The scintillometer measures the wind mainly in the central portion of the path. Consequently, when the scintillometers show higher winds than the ground stations, we infer that the winds are stronger in the center of the valley than on the sidewalls. This behavior is especially evident during the night, indicating the presence of a jet in the center of the valley.

### 3) COMPARISON WITH AIRCRAFT

The aircraft provides a possibility for comparing the scintillometer wind measurements with measurements done in the same atmospheric volume. Such comparisons were possible for the Castaneda and Santa Maria paths. Aircraft measurements made inside a box 200 m high and 1000 m wide, around the light paths, were selected for the comparisons. The aircraft flew typically a few minutes in the vicinity of the scintillometers, recording the wind speed at a rate of 0.25 Hz. Of the 150 data points sampled by the aircraft during a 10-min period, typically 20 data points were collected in the vicinity of the scintillometer; the maximum number of data points was 80. The average of these instantaneous measurements over a 10-min period are displayed in Fig. 14.

TABLE 5. Correlation between the scintillometer path at Pradiron and the ground stations in Pradiron (PRA) and Pian San Giacomo (PSG) (228 data points).

| | Slope | Peak | PRA | PSG |
|---|---|---|---|---|
| Slope | 1.00 | | | |
| Peak | 0.95 | 1.00 | | |
| PRA | 0.84 | 0.90 | 1.00 | |
| PSG | 0.90 | 0.92 | 0.86 | 1.00 |

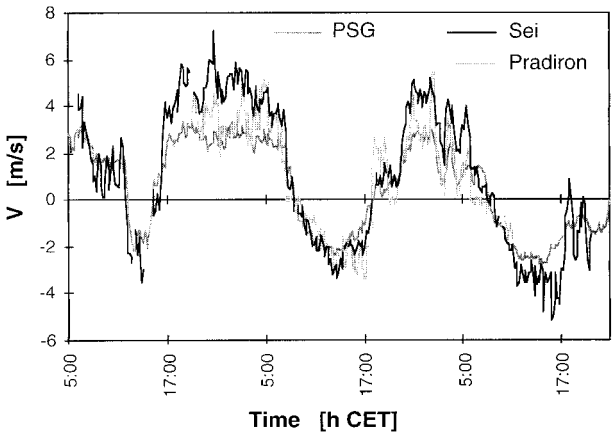


FIG. 13. Comparison of the Sei and Pradiron scintillometers with the ground station at Pian San Giacomo (PSG), 16–18 Aug 1996.

The comparisons show that the most common technique of evaluating crosswind (slope method) failed to provide the right crosswind speed but instead yielded values much too low. The peak technique, however, agrees fairly well with the aircraft measurements (Fig. 14). Consequently, for subsequent applications, we merged the peak and slope techniques in a ''covariance technique'' for which the wind speed is determined by the slope technique during night and transition periods and by the peak technique during the day. The reason for this problem is not yet fully understood but must be related to the fact that the Santa Maria and Castaneda paths are the longest and the highest above ground and therefore experience different turbulence structure than the Pradiron and Sei paths.

Aircraft measurements also show the inhomogeneity of the wind field over Grono. The wind profile sometimes shows a jet with higher wind speed on the east side of the valley.

### 4) COMPARISON WITH SODAR

A sodar was placed in San Vittore, at a distance of 3 km from the scintillometer paths of Santa Maria and Castaneda. In Figs. 15 and 16, the measurements made with the scintillometers in Castaneda and Santa Maria are compared to the measurements at the same elevation

TABLE 6. Correlation between the scintillometer paths at Santa Maria (SMA) and Castaneda (CAS) and the ground stations in Santa Maria and Grono (GRN) (228 data points).

| | SMA | GRN | Slope SMA | Peak SMA | Slope CAS | Peak CAS |
|---|---|---|---|---|---|---|
| SMA | 1.00 | | | | | |
| GRN | 0.68 | 1.00 | | | | |
| Slope SMA | 0.65 | 0.67 | 1.00 | | | |
| Peak SMA | 0.71 | 0.71 | 0.91 | 1.00 | | |
| Slope CAS | 0.61 | 0.59 | 0.70 | 0.75 | 1.00 | |
| Peak CAS | 0.65 | 0.67 | 0.76 | 0.83 | 0.86 | 1.00 |

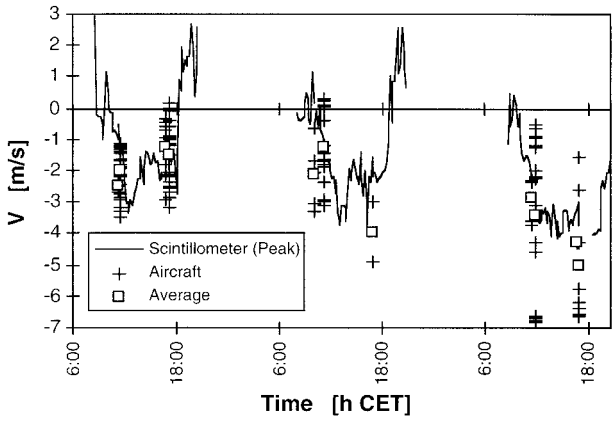


FIG. 14. Comparison between scintillometer and aircraft measurements, 16–18 Aug 1996. The aircraft measurements are taken from a box, 1 km long and 200 m high, around the light path. The crosses represent the instantaneous aircraft measurements, and the squares are averages of the aircraft measurements for 10-min periods.

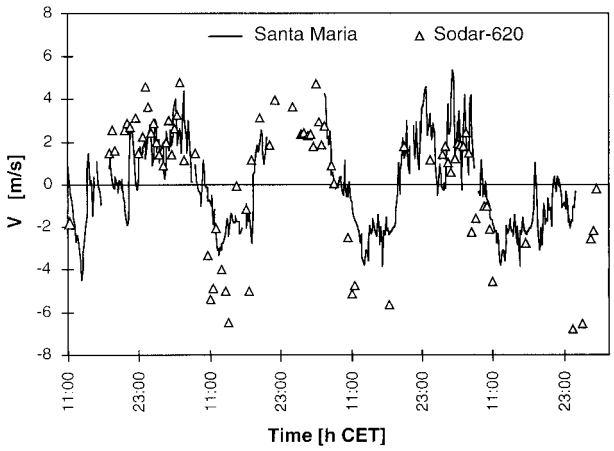


FIG. 16. Comparison between sodar, 620 m above ground, and scintillometer at Santa Maria (peak technique), 15–19 Aug 1996. Sodar measurements are 30-min averages, and scintillometer measurements are 10-min averages.

made by the sodar in San Vittore. During the night, both types of measurements agree fairly well, but the scintillometers show more variability because of their shorter averaging times.

During the day, the scintillometers show lower wind speeds than the sodar. During the up-valley wind phase, the aircraft data show a significant decrease in wind speed near Grono when compared to measurements near San Vittore. This trend was already visible in the ground station measurements, and this points toward a strong divergence of the wind field in the area of Grono. Although not yet completely understood, this phenomenon is important for determining the interaction between the valley circulation and the gradient wind aloft. A possible hypothesis is that the up-valley wind continues to flow east into a tributary valley where the air is forced to ascend. During the ascent, the air reaches the level of northerly flow and is deflected toward the southeast, definitively leaving the valley. Modeling studies may improve our understanding of this three-dimensional phenomenon.

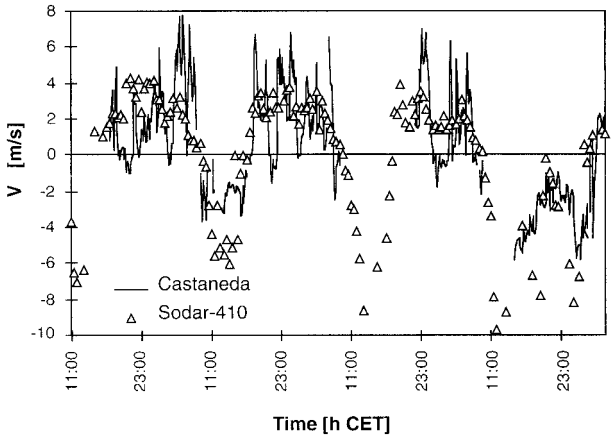


FIG. 15. Comparison between sodar, 410 m above ground, and scintillometer at Castaneda (peak technique), 15–19 Aug 1996. Sodar measurements are 30-min averages, and scintillometer measurement are 10-min averages.

### 5) SPECTRAL ANALYSES

Spectral analyses of the horizontal wind measurements are presented in Fig. 17. To produce these spectra, we analyzed data series of 15-s averages. We split each such time series, which was typically 10 h long, into blocks of 50 min; detrended each block; computed a spectrum for each; normalized each spectrum with its variance; then averaged all the blocks. In Fig. 17, the scintillometer winds show the typical $-\frac{5}{3}$ Kolmogorov inertial-subrange roll-off for about one frequency decade. Because of noise contamination (e.g., Fig. 7) and path averaging within the sample volume of the scintillometer (Andreas et al. 1992), the spectra in Fig. 17

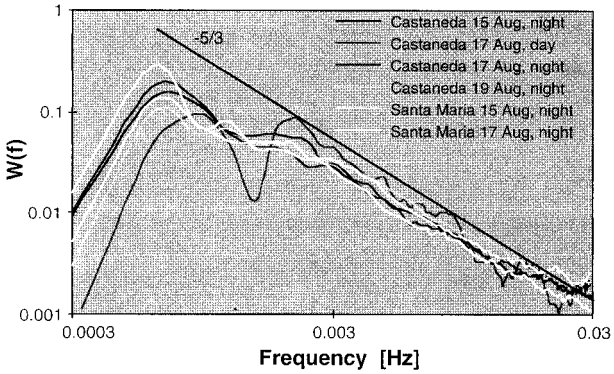


FIG. 17. Normalized wind spectra for Santa Maria and Castaneda on different days computed using the slope method with polynomial detrending over 50 min.

TABLE 7. Reliability of the different techniques for different periods of the day.

| | Daytime | Nighttime | Transition |
|---|---|---|---|
| Peak | Good | Good | Average |
| Slope | Average | Good | Average |
| Frequency | Good | Poor | Average |

contain no useful information at frequencies higher than about 0.03 Hz.

To our knowledge, these are the first spectra ever computed from crosswind scintillometer data. The reasonable shape of these spectra and their behavior in the inertial subrange are further evidence of the quality of our scintillometer crosswind measurements.

## 5. Conclusions

The loss of correlation of the scintillation pattern, as evidenced by values of the correlation function less than one, is not only due to inhomogeneities along the path, or the nonlinear interaction of large and small eddies, but also to violations of Taylor's hypothesis. The nonlinear relationship between the frequency of scintillation and the wind speed, (9), accounts for violations of Taylor's hypothesis.

For all paths, we can classify the measurement into day, transition, and night periods. During transition periods, the intensity fluctuations are very weak, the values of $C(\tau_p)$ get very low, and the scintillation is not sufficient to ensure a reliable wind measurement. The wind measurement is thus questionable for every technique. Specifically, during transition periods the peak technique and the frequency techniques give unrealistically high values. Failure of the slope technique during transition periods is less obvious because it gives a value that tends to zero, which corresponds, by chance, to the true wind speed. The performance of the different techniques is summarized in Table 7.

During the day, the intensity fluctuations are sufficient to ensure reliable measurements. The values of $C(\tau_p)$ depend on the wind speed, and the turbulence measurement is proportional to the incoming solar radiation. All the techniques agree fairly well with each other, except for the slope technique applied to the Santa Maria and Castaneda paths. The slope technique obviously gives values that are too low. This failure is probably due to the inhomogeneity of the atmosphere.

During the night, high levels of turbulence are measured. The frequency techniques fail to provide reasonable measurements most of the time. This problem seems to be related to changes in the turbulence spectrum. Another peculiarity of the night is that the scintillometers measure wind speeds that are significantly higher than the winds measured at the ground. This likely results because the higher atmosphere is frictionally decoupled from the stably stratified surface layer.

*Acknowledgments.* The authors want to thank René Richter and Robert Erne, as well as the whole atmospheric pollution section of PSI for their efforts during the measurement campaign. The scintillometer was developed with the collaboration of ELSYS AG. The excellent aircraft measurements were performed by MetAir AG, and the sodar measurements by the Institute of Meteorology and Physics of the Agricultural University of Vienna.

This VOTALP project was supported by the Swiss Federal Office for Education and Science, Grant 95.0386-2. The U.S. Department of the Army supported Ed Andreas's participation in this work.

REFERENCES

Andreas, E. L, 1991: Using scintillation at two wavelengths to measure path-averaged heat fluxes in free convection. *Bound.-Layer Meteor.*, **54,** 167–182.

——, J. R. Gosz, and C. N. Dahm, 1992: Can long-path FTIR spectroscopy yield gas flux measurements through a variance technique? *Atmos. Environ.*, **26A,** 225–233.

Biltoft, C. A., 1989: Field testing of a crosswind scintillometer. *Proc. SPIE*, **1115,** 167–178.

Briggs, B. H., G. J. Phillips, and D. H. Shinn, 1950: The analysis of observations on spaced receivers of the fading of radio signals. *Proc. Phys. Soc.*, **63B,** 106–121.

de Bruin, H. A. R., B. J. J. M. van den Hurk, and W. Kohsiek, 1995: The scintillation method tested over a dry vineyard area. *Bound.-Layer Meteor.*, **76,** 25–40.

de Jong, A., and G. de Leeuw, 1997: Low elevation transmission measurements at EOPACE; Part III: Scintillation effects. *Proc. SPIE*, **3125,** 135–147.

Eaton, F. D., W. A. Peterson, J. R. Hines, J. J. Drexler, D. B. Soules, A. H. Waldie, and J. A. Qualtrough, 1990: Morphology of atmospheric transparent inhomogeneities. *Proc. SPIE*, **1312,** 134–146.

Furger, M., A. Prévôt, L. P. Poggio, J. Dommen, and W. K. Graber, 1997: Observation of ozone transport in a valley in the Swiss Alps. Preprints, *12th Symp. on Boundary Layer and Turbulence*, Vancouver, BC, Canada, Amer. Meteor. Soc., 512–513.

Hill, R. J., 1996: Corrections to Taylor's frozen turbulence approximation. *Atmos. Res.*, **40,** 153–175.

——, 1997: Algorithms for obtaining atmospheric surface-layer fluxes from scintillation measurements. *J. Atmos. Oceanic Technol.*, **14,** 456–467.

Lawrence, R. S., G. R. Ochs, and S. F. Clifford, 1972: Use of scintillations to measure average wind across a light beam. *Appl. Opt.*, **11,** 239–243.

Porch, W. M., W. D. Neff, and C. W. King, 1988: Comparisons of meteorological structure parameters in complex terrain using optical and acoustical techniques. *Appl. Opt.*, **27,** 2222–2228.

Wang, T. I., and J. D. Crosby, 1996: Optical scintillometer to measure atmospheric turbulence and runway cross wind. Preprints, *Workshop on Wind Shear and Wind Shear Alert Systems*, Oklahoma City, OK, Amer. Meteor. Soc., 192–198.

——, G. R. Ochs, and R. S. Lawrence, 1981: Wind measurements by the temporal cross correlation of the optical scintillations. *Appl. Opt.*, **20,** 4073–4081.

Wotawa, G., and Coauthors, 1996: The EU Research Project VOTALP—Objectives and first results. *Proc. 24th Int. Conf. on Alpine Meteorology—ICAM'96*, Bled, Slovenia, Hydrometeorological Institute of Slovenia, 297–303.

Wyngaard, J. C., and S. F. Clifford, 1977: Taylor's hypothesis and high-frequency turbulence spectra. *J. Atmos. Sci.*, **34,** 922–929.